

Electrically-Driven and Exponentially-Enhanced Spin-Photon Interfaces for Quantum Networks

Fang-Yu Hong¹

¹*Zhejiang Key Laboratory of Quantum State Control and Optical Field Manipulation, Department of Physics, Zhejiang Sci-Tech University, Hangzhou, Zhejiang 310018, China*
(Dated: September 11, 2024)

We present an electrically-driven scheme for spin-photon quantum interfaces used in quantum networks. Through modulating the motion of a nano cantilever with voltages, optomechanical coupling and spin-mechanical coupling can be exponentially enhanced simultaneously. Numerical simulations show that by applying well-designed voltages high-fidelity quantum interface operations such as generation and absorption of a single-photon with a known wave packet are within the reach of current techniques.

PACS numbers: 03.67.Hk, 07.10.Cm, 42.50.Wk

Keywords: electrically-driven, quantum interface, optonanomechanics, state transfer

I. INTRODUCTION

Nitrogen-vacancy (NV) impurities in diamond are promising solid-state qubits for emerging quantum computation and quantum communication because of their long spin coherence times even at room temperature [1, 2] and fast manipulation speed [3], combined with a level structure allowing for straightforward optical initialization and readout of the electronic spin state [4]. Quantum networks comprised of local nodes and quantum channels are of fundamental importance for secure quantum communication [5], blind computing of both classical and quantum algorithms [6], and modular quantum computing [7, 8], timing [9], and sensing [10]. Quantum interfaces mapping between optical “flying” qubits and “stationary” qubits is an indispensable component of such a quantum network. Light-matter quantum interface protocols based on time-dependent laser pulses have been first described and carried out by atomic systems [11–17]. In each of these experiments or proposals, the quantum interface operations have to be carried out through precisely controlled laser pulses to modulate the light-matter interactions which have to be strong enough to reach the strong-coupling regime. Laser pulses are difficult to be produced on-chip and to be manipulated within a nanoscale region due to its diffraction effect. Thus from the viewpoint of practical application, it is worth developing an electrically driven [18–21] quantum interfaces for quantum networks

Recently several proposes [22–24] have been put forward to exponentially enhance spin-phonon coupling through modulating a spring constant of a mechanical cantilever with a time-dependent voltage. Here we show that by introducing a parametric drive (two-phonon drive) voltage to modulate a nano cantilever motion we can exponentially enhance optomechanical (OM) coupling and spin-mechanical (SM) coupling simultaneously. With this control at hand we design an electrically-driven scheme to fulfill many kind of quantum interface functions. Even under the conditions where the SM cou-

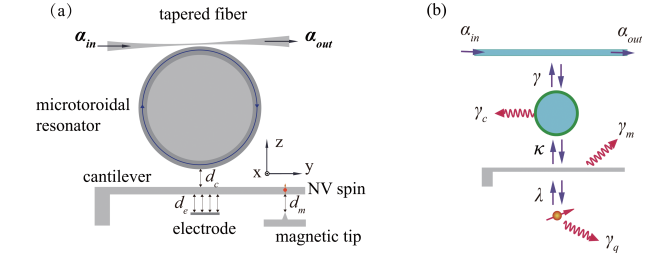


FIG. 1. (color online). (a) Schematic setup for a quantum light-matter interface. Driving voltage applied on the electrodes change the nano cantilever’s position, which modifies and enhances spin-mechanical interaction and optomechanical interaction simultaneously. Applying voltage pulses can accomplish the generation or absorption of a single-photon wavepacket, resulting in a state transfer or an entanglement distribution between two remote quantum nodes. (b) The interactions among the components of a quantum interface, and corresponding decoherence sources

pling and the OM coupling are not satisfied with the strong coupling regime many quantum interface operations such as generating/absorbing a single-photon and establish spin-photon entanglement can still be accomplished with high fidelity.

II. EXPONENTIALLY ENHANCED COUPLINGS

The prototype quantum interface consists of a high-Q microtoroidal resonator, a nano cantilever with effective mass M and vibration frequency ω_m , an optical waveguide (e.g., a tapered fiber), and a NV center embedded in the cantilever shown in Fig. 1(a). To control the motion of the cantilever, a tunable time-varying voltage $V = V_0 + V_p \cos(2\omega_p t)$ is applied on a pair of electrodes of area A , one of which is coated on the lower surface of the cantilever [22, 24]. The spring constant of the cantilever can be regulated through the gradient of the

electrostatic force $F = \partial(C_r V^2)/2\partial z$ with the parallel-plate capacitor $C_r = \epsilon A/(d_e + z)$ of the two electrodes, where z denotes the modulated part of the distance relative to the equilibrium d_e between the two electrodes. Under the electrical drive the cantilever motion can be modeled by a Hamiltonian ($\hbar = 1$) [25]

$$H_m = \omega_m \hat{a}^\dagger \hat{a} - \Omega_p \cos(2\omega_p t) (\hat{a} + \hat{a}^\dagger)^2, \quad (1)$$

where

$$\Omega_p = -\frac{\epsilon A V_0 V_p a_0^2}{\hbar d_e^3} \quad (2)$$

with the zero-point fluctuation $a_0 = \sqrt{\hbar/2M\omega_m}$ and the corresponding annihilation operator \hat{a} .

The electronic ground state of the NV spin qubit is a $S = 1$ spin triplet labeled by $|m_s\rangle$ with $m_s = 0, \pm 1$. Two microwave (mw) fields with the same Rabi frequency Ω and the same detuning Δ drive oscillations between $|0\rangle$ and $|\pm 1\rangle$. The NV symmetry axis is assumed to be aligned along the z axis. Motion of the cantilever exposes the NV spin to a magnetic field $|B_{\text{tip}}| \simeq G_m \hat{z}$ produced by a nearby magnetic tip, which is proportional to the position operator $\hat{z} = a_0(\hat{a} + \hat{a}^\dagger)$ and leads to a Hamiltonian [26]

$$H_{\text{mq}} = \omega_m \hat{a}^\dagger \hat{a} + \omega_e |e\rangle\langle e| + \omega_q |d\rangle\langle d| + (\lambda |g\rangle\langle d| + \lambda_e |d\rangle\langle e| + \text{H.c.}) (\hat{a} + \hat{a}^\dagger) - \Omega_p \cos(2\omega_p t) (\hat{a} + \hat{a}^\dagger)^2, \quad (3)$$

where $|e\rangle = \cos(\theta)(|-1\rangle + |1\rangle)/\sqrt{2} + \sin(\theta)|0\rangle$, $|g\rangle = \cos(\theta)|0\rangle - \sin(\theta)(|-1\rangle + |1\rangle)/\sqrt{2}$, $|d\rangle = (|-1\rangle - |1\rangle)/\sqrt{2}$, $\omega_q = \omega_d - \omega_g$, and $\omega_e = \omega_f - \omega_g$, $\lambda = -\lambda_0 \sin(\theta)$, and $\lambda_e = \lambda_0 \cos(\theta)$, with $\tan(2\theta) = -\sqrt{2}\Omega/\Delta$, the corresponding eigenfrequencies $\omega_d = -\Delta$, and $\omega_{f/g} = (-\Delta \pm \sqrt{\Delta^2 + 2\Omega^2})/2$. Here $\lambda_0 = g_s \mu_B G_m a_0$ with $g_s \simeq 2$, and μ_B is the Bohr magneton.

Using a rotating transformation $U_0(t) = e^{-iH_0 t}$ with $H_0 = \omega_p \hat{a}^\dagger \hat{a}$ and dropping the high frequency oscillation and the constant items, the above Hamiltonian (3) can be rewritten as

$$\tilde{H}_{\text{mq}} = \delta_m \hat{a}^\dagger \hat{a} + \omega_e |e\rangle\langle e| + \omega_q |d\rangle\langle d| + (\lambda |g\rangle\langle d| + \lambda_e |d\rangle\langle e| + \text{H.c.}) (\hat{a} + \hat{a}^\dagger) - \frac{\Omega_p}{2} (\hat{a}^{\dagger 2} + \hat{a}^2), \quad (4)$$

where $\delta_m = \omega_m - \omega_p$.

Meanwhile the cantilever is coupled to a tightly confined optical modes of frequency ω_c of the microtoroidal cavity through its evanescent field with the single-photon OM coupling rate [16, 27, 28]

$$\kappa_0 = a_0 (\partial \omega_c / \partial d_c), \quad (5)$$

where d_c denotes the distance of the cantilever to the toroid. Since the scattering between two counterpropagating modes can be negligible by positioning the cantilever tangentially to the optical whispering-gallery mode trajectory as in Fig. 1a [16, 27, 29], here only a

forward circulating cavity mode is considered, which is coupled to the field in the tapered fiber with a constant $\sqrt{\gamma/2\pi}$ [30]. The optical field in the tapered fiber can be efficiently coupled to the toroidal microcavity mode which is then coupled back to the forward-propagating field in the fiber with an ideality greater than 99.97%, which is defined as the ratio of the amount of power coupled into the desired mode to that coupled into all modes [31]. The quantum interface can thus be modeled by a Hamiltonian [16, 22, 24, 27, 32]

$$H = H_{\text{mqc}} + H_{\text{cf}}, \quad (6)$$

where

$$H_{\text{mqc}} = \tilde{H}_{\text{mq}} + \Delta_{c0} \hat{c}^\dagger \hat{c} + \kappa_0 \hat{c}^\dagger \hat{c} (\hat{a} + \hat{a}^\dagger) + i[\varepsilon(t) \hat{c}^\dagger - \varepsilon(t)^* \hat{c}] \quad (7)$$

and

$$H_{\text{cf}} = \int_0^\infty \Delta_\omega \hat{f}_\omega^\dagger \hat{f}_\omega d\omega + \int_0^\infty \left(\sqrt{\frac{\gamma}{2\pi}} (\hat{c} \hat{f}_\omega^\dagger + \hat{c}^\dagger \hat{f}_\omega) \right) d\omega. \quad (8)$$

Here \hat{f}_ω is the annihilation operator for the mode of frequency ω in the optical channel and \hat{c} is the annihilation operators for the cavity modes of frequency ω_c , and $\varepsilon(t)$ is the slowly varying strength of an external laser field of frequency ω_L , which coherently excites the cavity field. The detuning parameters $\Delta_{c0} = \omega_c - \omega_L$ and $\Delta_\omega = \omega - \omega_L$. The driving laser field can be sent to the cavity via the tapered fiber shown in Fig.1.

In typical experiments the OM coupling κ_0 is too small to coherently manipulate the OM system. To achieve a considerable and tunable coupling a strongly driven OM system is widely adopted where the effective OM coupling is enhanced by the coherent field amplitude inside the cavity [16, 27, 28, 33]. The dissipative dynamics of the cavity field and the cantilever can be treated in terms of quantum Langevin equations (QLE) [29],

$$\dot{\hat{c}} = -i[\hat{c}, H_{\text{mqc}}] - \gamma_t \hat{c} - \sqrt{2\gamma} \hat{f}_{in}(t) - \sqrt{2\gamma_0} \hat{f}_0(t), \quad (9)$$

and

$$\dot{\hat{b}} = -i[\hat{b}, H_{\text{mqc}}] - \gamma_{m0} \hat{b} - \sqrt{\gamma_{m0}} \hat{\xi}(t). \quad (10)$$

Here $\gamma_t = \gamma + \gamma_0$ is the total decay rate, γ_0 is the additional intrinsic losses of the optical cavity mode, $\hat{f}_{in}(t)$ is the input field operator, $\hat{f}_0(t)$ is the associated noise operator, $\gamma_{m0}/2$ is the decay rate of the mechanical amplitude, and $\hat{\xi}(t)$ is a thermal white-noise operator satisfying $\langle \hat{\xi}(t) \hat{\xi}^\dagger(t') \rangle = (N_m + 1) \delta(t - t')$ and $[\hat{\xi}(t), \hat{\xi}^\dagger(t')] = \delta(t - t')$. Here N_m denotes the Bose occupation number for a mode of frequency ω_m . In the high-temperature case, $k_B T \gg \hbar \omega_m$, the corresponding thermal decoherence rate should be replaced by $\gamma_m \equiv \gamma_{m0} N_m \approx \frac{k_B T}{\hbar Q}$, where $Q = \omega_m / \gamma_{m0}$ is the quality factor of the mechanical resonance.

Beginning with QLEs (9) and (10), we implement a unitary transformation $\hat{c} \rightarrow \hat{c} + \tilde{c}$ and $\hat{a} \rightarrow \hat{a} + \tilde{a}$ such that the c number \tilde{c} and \tilde{a} denote the classical mean values of the modes and the new operators \hat{c} and \hat{a} delineate the quantum fluctuations around them. We require all the classical contributions to the transformed QLEs disappear, which gives

$$\dot{\tilde{c}} = -(i\Delta_{c0} + \gamma_t)\tilde{c} - i\kappa_0(\tilde{a} + \tilde{a}^*)\tilde{c} + \xi(t), \quad (11)$$

$$\dot{\tilde{a}} = -(i\delta_m + \frac{\gamma_{m0}}{2})\tilde{a} - i\kappa_0|\tilde{c}|^2 + i\Omega_p\tilde{a}^*. \quad (12)$$

For $\xi(t) = \text{const}$ and $\gamma_{m0} \rightarrow 0$ ($\gamma_m = \text{const}$) we have the steady-state solution

$$\tilde{a} = \frac{\kappa_0|\tilde{c}|^2}{\Omega_p - \delta_m} \quad (13)$$

with \tilde{c} determined from

$$\tilde{c} = \frac{\xi}{i\Delta_{c0} + \gamma_t + 2i\kappa_0^2|\tilde{c}|^2/(\Omega_p - \delta_m)}. \quad (14)$$

This formula still approximately holds if $\xi(t)$ is slowly varying compared to the characteristic response time, $\dot{\xi}(t)/\xi(t) \ll \gamma_t, \Delta_c, \delta_m$ for the case $|\tilde{c}|\kappa_0 \ll \Delta_c, \Omega_p - \delta_m$. Through Eq.(14) the applied laser power and phase can be related to a desired temporal profile $\tilde{c}(t)$.

In the strong driving regime where $|\tilde{c}(t)|^2 \gg 1$ we can linearize the OM coupling of Eq.(7): Going back to the displaced operators in the QLEs (9) and (10) and deleting the classical forces, the terms of order κ_0 relative to those of order $\kappa_0|\tilde{c}|$ and $\kappa_0|\tilde{c}|^2$ can be omitted. The result of this procedure can also be obtained by replacing H_{mqc} with the linearized OM Hamiltonian

$$H_{\text{mqc}}^{\text{lin}} = \tilde{H}_{\text{mqc}} + \Delta_c \hat{c}^\dagger \hat{c} + (\kappa \hat{c}^\dagger + \kappa \hat{c}^*)(\hat{a} + \hat{a}^\dagger) \quad (15)$$

with the laser-enhanced OM coupling $\kappa = \kappa_0 \tilde{c}(t)$ and the renormalized cavity detuning $\Delta_c = \Delta_{c0} + 2|\kappa(t)|^2/(\Omega_p - \delta_m)$

To diagonalize the mechanical mode of Hamiltonian $H^{\text{lin}} = H_{\text{mqc}}^{\text{lin}} + H_{\text{cf}}$ we take the unitary Bogoliubov transformation $U_S(r(t)) = \exp[r(t)(\hat{a}^2 - \hat{a}^{\dagger 2})/2]$ with the squeezing parameter $r(t)$ defined by $\tanh 2r(t) = \Omega_p(t)/\delta_m(t)$, leading to the Hamiltonian

$$\begin{aligned} H^S &= \omega_e |e\rangle\langle e| + \omega_q |d\rangle\langle d| + \Delta_m \hat{a}^\dagger \hat{a} + \Delta_c \hat{c}^\dagger \hat{c} \\ &+ \int_0^\infty \Delta_\omega \hat{f}_\omega^\dagger \hat{f}_\omega d\omega + \int_0^\infty \left(\sqrt{\frac{\gamma}{2\pi}} (\hat{c} \hat{f}_\omega^\dagger + \hat{c}^\dagger \hat{f}_\omega) \right) d\omega \\ &+ (\lambda_{\text{ef}} |g\rangle\langle d| + \lambda_e e^{r(t)} |d\rangle\langle e| + \text{H.c.})(\hat{a} + \hat{a}^\dagger) \\ &+ (\kappa_{\text{ef}} \hat{c}^\dagger + \kappa_{\text{ef}} \hat{c})(\hat{a} + \hat{a}^\dagger) + \frac{i}{2} \dot{r}(t)(\hat{a}^2 - \hat{a}^{\dagger 2}), \quad (16) \end{aligned}$$

where $\Delta_m = \delta_m / \cosh 2r(t)$, $\lambda_{\text{ef}} = \lambda e^{r(t)}$, and $\kappa_{\text{ef}} = \kappa e^{r(t)}$ with λ and κ assuming to be real. Applying a unitary transformation $U = \exp(i\pi|d\rangle\langle d|/2 + i\pi\hat{c}^\dagger \hat{c}/2)$ and the

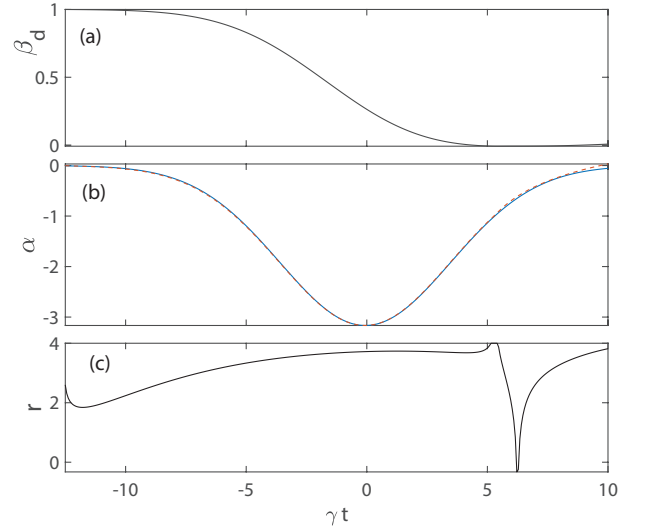


FIG. 2. (Color online). Numerical simulation of generating a single-photon. The parameters used are $\gamma/2\pi = 10\text{MHz}$, $\kappa/2\pi = 0.09\text{MHz}$, $\lambda/2\pi = 0.05\text{MHz}$, $\gamma_c = 0.01\gamma$, $\gamma_m = 0.01\lambda$, and $\gamma_q/2\pi = 2\text{kHz}$. (a) The evolution of state amplitude $\beta_d(t)$. (b) The ideal single-photon wavepacket $\alpha_{\text{out}}^{\text{ideal}}(t) = \tilde{\alpha}(t)$ (solid line) and the generated single-photon wavepacket α_{out} (dashed line). (c) The driving squeezing parameter r .

rotating-wave approximation (RWA) with the resonance condition $\Delta'_m \equiv -\Delta_m \approx \Delta_c \approx \omega_q \neq \omega_e$ Hamiltonian (16) reduces to

$$\begin{aligned} H^S_{\text{rwa}} &= \frac{\omega_q}{2} \hat{\sigma}_z + \Delta_m \hat{a}^\dagger \hat{a} + \Delta_c \hat{c}^\dagger \hat{c} + \int_0^\infty \Delta_\omega \hat{f}_\omega^\dagger \hat{f}_\omega d\omega + \\ &i \left(\lambda_{\text{ef}} \hat{\sigma}_+ \hat{a}^\dagger + \kappa_{\text{ef}} \hat{c}^\dagger \hat{a}^\dagger + \sqrt{\frac{\gamma}{2\pi}} \int_0^\infty \hat{c}^\dagger \hat{f}_\omega d\omega - \text{H.c.} \right) \quad (17) \end{aligned}$$

where $\hat{\sigma}_z$ is the Pauli operator and $\hat{\sigma}_+ = |d\rangle\langle g|$ is the raising operator for the spin qubit. Note that we work in the regime where $\Delta_m < 0$, for the sake of convenience Hamiltonian (17) can be rewritten as

$$\begin{aligned} H^S_{\text{f}} &= \frac{\omega_q}{2} \hat{\sigma}_z + \Delta'_m \hat{a}_m^\dagger \hat{a}_m + \Delta_c \hat{c}^\dagger \hat{c} + \int_0^\infty \Delta_\omega \hat{f}_\omega^\dagger \hat{f}_\omega d\omega + \\ &i \left(\lambda_{\text{ef}} \hat{\sigma}_+ \hat{a}_m + \kappa_{\text{ef}} \hat{c}^\dagger \hat{a}_m + \sqrt{\frac{\gamma}{2\pi}} \int_0^\infty \hat{c}^\dagger \hat{f}_\omega d\omega - \text{H.c.} \right) \quad (18) \end{aligned}$$

where $\hat{a}_m = \hat{a}^\dagger$ and the constant energy has been omitted. The coupling strength λ_{ef} and κ_{ef} are both exponentially enhanced simultaneously because of the modulating parametric driving voltage applied on the cantilever.

III. QUANTUM INTERFACE CONTROL SCHEME

Under the RWA which holds if $\lambda_{\text{ef}}, \kappa_{\text{ef}}, \dot{r}/2 \ll \omega_q + \Delta_c$ the probability of generating more than one exciton is negligible. Throughout the whole process of interconverting local and flying qubits in the quantum interface,

the state $|g, 0, 0\rangle|vac\rangle$ does not evolve into the subspace spanned by basis $|d, 0, 0\rangle|vac\rangle$, $|g, 1, 0\rangle|vac\rangle$, $|g, 0, 1\rangle|vac\rangle$, and $\hat{f}_\omega^\dagger|g, 0, 0\rangle|vac\rangle$, where $|vac\rangle$ is the vacuum state of the flying qubit, and in notations $|u, j, k\rangle$, $u = g, d$ denotes the stationary qubit states, j, k denote the number of excitations in the mechanical and cavity mode, respectively. Hence, in the interaction picture the evolution of the system are in the form $|\Psi\rangle = C_g|g, 0, 0\rangle|vac\rangle + C_d|\Psi^d(t)\rangle$, where

$$|\Psi^d(t)\rangle = \int_0^\infty d\omega \alpha_\omega \hat{f}_\omega^\dagger |g, 0, 0\rangle|vac\rangle + \beta_d |d, 0, 0\rangle|vac\rangle + \beta_m |g, 1, 0\rangle|vac\rangle + \beta_c |g, 0, 1\rangle|vac\rangle. \quad (19)$$

Under the Hamiltonian given in Eq.(18), the Schrödinger equations for the state amplitudes of the quantum interface system in the interaction picture can be derived as

$$\dot{\beta}_d = \lambda_{ef} \beta_m e^{-i(\Delta'_m - \omega_q)t}, \quad (20a)$$

$$\dot{\beta}_m = -\lambda_{ef} \beta_d e^{i(\Delta'_m - \omega_q)t} - \kappa_{ef} \beta_c e^{i(\Delta'_m - \Delta_c)t}, \quad (20b)$$

$$\dot{\beta}_c = \kappa_{ef} \beta_m e^{-i(\Delta'_m - \Delta_c)t} + \sqrt{\frac{\gamma}{2\pi}} \int_0^\infty \alpha_\omega e^{-i(\Delta_\omega - \Delta_c)t} d\omega, \quad (20c)$$

$$\dot{\alpha}_\omega = -\sqrt{\frac{\gamma}{2\pi}} \beta_c e^{i(\Delta_\omega - \Delta_c)t}. \quad (20d)$$

Integrating equation (20d) yields

$$\alpha_\omega(t) = \alpha_\omega(t_0) - \sqrt{\frac{\gamma}{2\pi}} \int_{t_0}^t e^{i(\Delta_\omega - \Delta_c)t'} \beta_c(t') dt', \quad (21)$$

or

$$\alpha_\omega(t) = \alpha_\omega(t_1) + \sqrt{\frac{\gamma}{2\pi}} \int_t^{t_1} e^{i(\Delta_\omega - \Delta_c)t'} \beta_c(t') dt', \quad (22)$$

where $t_0 \rightarrow -\infty$ and $t_1 \rightarrow \infty$ denote the remote past and remote future respectively when the incoming/outgoing photon wavepackets are not influenced by the quantum interface.

By substituting equation (21) or (22) into equation (20c) and applying the Weisskopf-Wigner approximation [34] the Schrödinger equations (20) can be rewritten as

$$\dot{\beta}_d = \lambda_{ef} \beta_m e^{-i(\Delta'_m - \omega_q)t}, \quad (23a)$$

$$\dot{\beta}_m = -\lambda_{ef} \beta_d e^{i(\Delta'_m - \omega_q)t} - \kappa_{ef} \beta_c e^{i(\Delta'_m - \Delta_c)t}, \quad (23b)$$

$$\begin{aligned} \dot{\beta}_c &= \kappa_{ef} \beta_m e^{-i(\Delta'_m - \Delta_c)t} - \sqrt{\gamma} \alpha_{in}(t) - \frac{\gamma}{2} \beta_c, \quad (23c) \\ &= \kappa_{ef} \beta_m e^{-i(\Delta'_m - \Delta_c)t} - \sqrt{\gamma} \alpha_{out}(t) + \frac{\gamma}{2} \beta_c, \end{aligned} \quad (23d)$$

where $\alpha_{in}(t) \equiv \int d\omega \alpha_\omega(t_0) e^{i(\Delta_c - \Delta_\omega)t} / \sqrt{2\pi}$ with $t_0 \rightarrow -\infty$ and $\alpha_{out}(t) \equiv \int d\omega \alpha_\omega(t_1) e^{i(\Delta_c - \Delta_\omega)t} / \sqrt{2\pi}$ with $t_1 \rightarrow +\infty$ are the incoming and outgoing photon pulses in the quantum channel, respectively.

According to equations (23c) and (23d) the solution for β_c is

$$\beta_c(t) = \frac{1}{\sqrt{\gamma}} \left(\alpha_{out}(t) - \alpha_{in}(t) \right). \quad (24)$$

Substituting equation (23c) into equation (23a) gives

$$\dot{\beta}_d(t) = \frac{\lambda}{\kappa} \left(\dot{\beta}_c + \sqrt{\gamma} \alpha_{in}(t) + \frac{\gamma}{2} \beta_c \right) e^{i(\omega_q - \Delta_c)t}. \quad (25)$$

From equations (23) the normalization condition can be derived as follows

$$\frac{d}{dt} (|\beta_d|^2 + |\beta_m|^2 + |\beta_c|^2) = |\alpha_{in}(t)|^2 - |\alpha_{out}(t)|^2. \quad (26)$$

From Eq.(23b) we have

$$\begin{aligned} |\beta_m|^2 \frac{d}{dt} \theta_m &= i \left(-|\dot{\beta}_m| |\beta_m| + \lambda_{ef} \beta_d \beta_m^* e^{i(\Delta'_m - \omega_q)t} \right. \\ &\quad \left. + \kappa_{ef} \beta_c \beta_m^* e^{i(\Delta'_m - \Delta_c)t} \right) \end{aligned} \quad (27)$$

with $\theta_m = \arg(\beta_m)$. From Eq. (27) and Eq. (23a) we have

$$\frac{d}{dt} \theta_m = \frac{i}{2|\beta_m|^2} \left(\beta_d \dot{\beta}_d^* + \frac{\kappa}{\lambda} \beta_c \dot{\beta}_d^* e^{i(\Delta_c - \omega_q)t} - \text{c.c.} \right), \quad (28)$$

where ‘c.c.’ denotes complex conjugate.

At last from equation (23c), we get the squeezing parameter r

$$e^r = \frac{1}{\kappa \beta_m} \left(\dot{\beta}_c + \sqrt{\gamma} \alpha_{in}(t) + \frac{\gamma}{2} \beta_c \right) e^{i(\Delta'_m - \Delta_c)t}. \quad (29)$$

For simplicity $\alpha_{out}(t)$ and $\alpha_{in}(t)$ are both assumed to be real and the resonance condition $\Delta'_m = \Delta_c = \omega_q$ is satisfied. The quantum interface can be designed in this way: first, the wave packets of the outgoing/incoming single-photon are arbitrarily assigned only if they are sufficiently smooth; the evolution of cavity mode $\beta_c(t)$ is then determined according to Eq. (24); third, the state amplitudes β_d can be solved from Eq. (25); next the evolution of β_m can be obtained from equations (26) and (28); and the squeezing parameter r can be determined according to Eq. (29) with $\Delta'_m = \Delta_c$; at last we choose appropriate parameters such as ω_p , Δ , and Ω to satisfy the resonance condition

$$\frac{\omega_p(t) - \omega_m}{\cosh(2r(t))} = \Delta_c = \omega_q. \quad (30)$$

For the sending node of a quantum network, the initial conditions are $\alpha_{in}(t) = 0$, $\beta_d(t_0) = 1$, $\beta_m(t_0) = 0$, $\beta_c(t_0) = 0$. The outgoing single-photon wave packet can contain average $\sin^2 \varphi$ photon with a single-photon wavepacket $\tilde{\alpha}(t)$: $\int_{t_0}^{t_1} dt |\alpha_{out}(t)|^2 = \sin^2 \varphi \int_{t_0}^{t_1} dt |\tilde{\alpha}(t)|^2 = \sin^2 \varphi$. At the remote future time $t_1 \rightarrow +\infty$, the photon

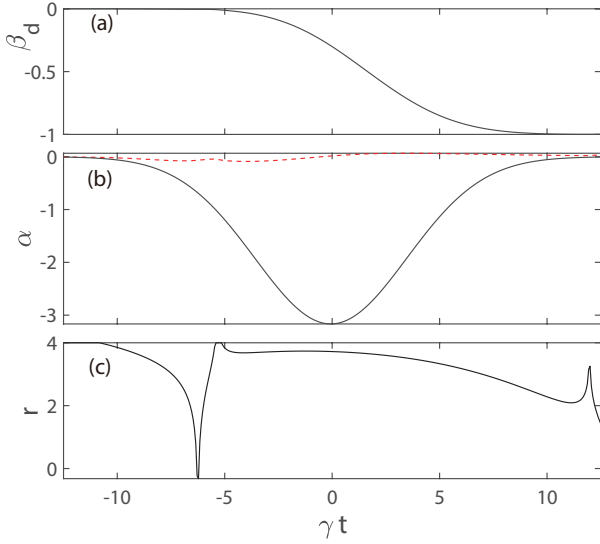


FIG. 3. (Color online). Numerical simulation of absorbing a single-photon wavepacket. The parameters used are as those in Fig. 2. (a) The evolution of state amplitude $\beta_d(t)$. (b) The incoming single-photon wavepacket $\alpha_{in}(t) = \tilde{\alpha}(t)$ (solid line) and the reflected photon wavepacket (dashed line). (c) The driving squeezing parameter r .

generation process is completed, we have $\beta_m(t_1) = 0$, $\beta_c(t_1) = 0$, and $\beta_d(t_1) = \cos \varphi e^\phi$ with the phase ϕ determined by Eq. (25). The most general form of the photon generation process in the quantum interface can be described by [13]

$$C_g |g, 0, 0\rangle|vac\rangle + C_d |d, 0, 0\rangle|vac\rangle \xrightarrow{r(t)} C_g |g, 0, 0\rangle|vac\rangle + C_d [e^\phi \cos \varphi |d, 0, 0\rangle|vac\rangle + \sin \varphi |g, 0, 0\rangle|\tilde{\alpha}(t)\rangle]. \quad (31)$$

If $\varphi = \pi/2$, Eq. (31) is reduced to

$$C_g |g, 0, 0\rangle|vac\rangle + C_d |d, 0, 0\rangle|vac\rangle \xrightarrow{r(t)} |g, 0, 0\rangle[C_g|vac\rangle + C_d|\tilde{\alpha}(t)\rangle], \quad (32)$$

mapping the stationary qubit state onto the flying qubit. Further, if initially the qubit is in state $|d\rangle$, then this mapping operation can work as the deterministic generation of a single-photon with any desired pulse shape $\tilde{\alpha}(t)$. If $\varphi < \pi/2$, this sending node can also work as generating entanglement between the stationary qubit and the flying qubit:

$$|d, 0, 0\rangle|vac\rangle \xrightarrow{r(t)} e^\phi \cos \varphi |d, 0, 0\rangle|vac\rangle + \sin \varphi |g, 0, 0\rangle|\tilde{\alpha}(t)\rangle. \quad (33)$$

The receiving process is basically the time reversal of the sending process under the condition $\varphi = \pi/2$ [13]. With the qubit initially in state $|g\rangle$ and the incoming flying qubit in state $C_g|vac\rangle + C_d|\tilde{\alpha}(t)\rangle$, the mapping transformation is

$$|g, 0, 0\rangle(C_g|vac\rangle + C_d|\tilde{\alpha}(t)\rangle) \xrightarrow{r(t)} (C_g|g, 0, 0\rangle|vac\rangle - C_d|d, 0, 0\rangle|vac\rangle), \quad (34)$$

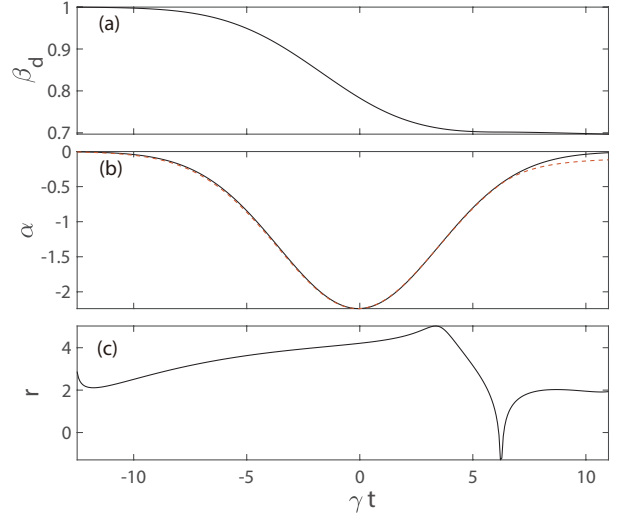


FIG. 4. (Color online). Establishing entanglement $|\psi\rangle = \frac{1}{\sqrt{2}}(|d\rangle|vac\rangle + |g\rangle|\tilde{\alpha}(t)\rangle)$ between a spin qubit and a single-photon. The corresponding parameters remain the same as those in figure 2 except $\lambda/2\pi = 0.02$ MHz. (a) The evolution of state amplitude $\beta_d(t)$. (b) The ideal single-photon wavepacket $\alpha_{out}^{ideal}(t) = \frac{1}{\sqrt{2}}\tilde{\alpha}(t)$ (solid line) and the generated single-photon wavepacket α_{out} (dashed line). (c) The driving squeezing parameter r .

followed by a unitary transformation $U_2 = \begin{bmatrix} 1 & 0 \\ 0 & -1 \end{bmatrix}$ on the spin qubit in the receiving node to accomplish a state transfer $C_g|g\rangle_1 + C_d|d\rangle_1 \rightarrow C_g|g\rangle_2 + C_d|d\rangle_2$ with subscript $i = 1, 2$ represents the spin qubit in the sending/receiving node, respectively. By combining the sending and receiving process, the transfer of an arbitrary unknown qubit state from one node to another can be accomplished. When two neighboring nodes carry out state transfer operations followed by receiving state operation at the same time, the two qubits states are swapped. If $\varphi < \pi/2$ for the sending node, the joint operation of the sending and receiving process can generate an entanglement between two remote nodes by transformation

$$|d\rangle_1|vac\rangle|g\rangle_2 \xrightarrow[r_2(t)]{r_1(t)} (e^\phi \cos \varphi |d\rangle_1|g\rangle_2 - \sin \varphi |g\rangle_1|d\rangle_2)|vac\rangle, \quad (35)$$

with the corresponding squeezing parameters $r_i(t)$ ($i = 1, 2$) for the sending / receiving node, respectively.

IV. NUMERICAL SIMULATION AND DISCUSSION

Now we discuss the effects arising from some inevitable decoherence sources. In the high-temperature situation where $k_B T \gg \hbar\omega_m$, the effective mechanical dissipation rate $\gamma_m \approx \frac{k_B T}{\hbar Q}$ [16]. When the coupling rates λ_{ef} and κ_{ef} are exponentially enhanced, so does the effective cantilever decoherence rate. But the harmful effect of ampli-

fied mechanical noises can be circumvent by applying the experimentally accomplished dissipative squeezing technique [35–37], in which the Bogoliubov mode can be kept in its ground state [38].

Taking into account the decoherence including the photon leakage into free space (with rate γ_c) and that from the cantilever and the spin qubit (with rate γ_q) the Schrödinger equations (23) should be replaced by

$$\dot{\beta}_d = \lambda_{\text{ef}}\beta_m - \frac{\gamma_q}{2}\beta_d, \quad (36a)$$

$$\dot{\beta}_m = -\lambda_{\text{ef}}\beta_d - \kappa_{\text{ef}}\beta_c - \frac{\gamma_m}{2}\beta_m, \quad (36b)$$

$$\dot{\beta}_c = \kappa_{\text{ef}}\beta_m - \sqrt{\gamma}\alpha_{\text{in}}(t) - \left(\frac{\gamma}{2} + \frac{\gamma_c}{2}\right)\beta_c, \quad (36c)$$

$$= \kappa_{\text{ef}}\beta_m - \sqrt{\gamma}\alpha_{\text{out}}(t) + \left(\frac{\gamma}{2} - \frac{\gamma_c}{2}\right)\beta_c, \quad (36d)$$

where for the sake of simplicity, we have assumed the resonance conditions $\Delta'_m = \omega_q = \Delta_c$.

The scheme is to design the squeezing parameter $r(t)$ according to equation (29) through assigning target single-photon wavepacket $\alpha_{\text{in}}(t)$ or $\alpha_{\text{out}}(t)$, and use it to drive equations (36) under the real situation. First we simulate generating a single-photon wavepacket $\alpha_{\text{out}}^{\text{ideal}}(t) = \tilde{\alpha}(t) \equiv -\exp(-(\gamma t/5)^2)$ with normalization understood, under the driving voltage applied on the electrodes, which is dependent on the squeezing parameter r shown in Fig. 2(c), the evolution of the whole quantum interface can be obtained, here we plot the evolution of amplitude of the state β_d in Fig. 2(a) and the generated single-photon wavepacket α_{out} in Fig. 2(b) (dashed line). In the simulation we have used the corresponding parameters $\lambda/2\pi = 0.05$ MHz, $\kappa/2\pi = 0.09$ MHz, $\gamma/2\pi = 10$ MHz, $\gamma_c = 0.01\gamma$, $\gamma_m = 0.01\lambda$, and $\lambda_q/2\pi = 2$ kHz. The single photon generation fidelity $\langle \alpha_{\text{out}}^{\text{ideal}} | \alpha_{\text{out}} \rangle = 0.9879$. If we increase the mechanical decoherence rate to $\gamma_m = \lambda$, the fidelity slightly decrease to 0.9760.

Next we simulate absorbing a single-photon wavepacket $\alpha_{\text{in}}^{\text{ideal}}(t) = \tilde{\alpha}(t)$ shown in Fig. 3. The photon absorption fidelity is $\beta_d^{\text{ideal}}(t_1)\beta_d(t_1) = 0.9869$ with $\beta_d^{\text{ideal}}(t_1) = -1$ and the probability of an incoming single-photon wavepacket being reflected is $\int |\alpha_{\text{out}}(t)|^2 dt = 0.11\%$. Figure 4 shows establishing entanglement between a spin qubit and a flying qubit through generating a photon wavepacket $\alpha_{\text{out}}^{\text{ideal}}(t) = \frac{1}{\sqrt{2}}\tilde{\alpha}(t)$. The fidelity of establishing spin-photon entanglement is $\langle \alpha_{\text{out}}^{\text{ideal}} | \alpha_{\text{out}} \rangle + \beta_d^{\text{ideal}}(t_1)\beta_d(t_1) = 0.9841$ with $\beta_d^{\text{ideal}}(t_1) = \frac{1}{\sqrt{2}}$. All those operations can be finished within $0.4\mu\text{s}$. Note that in all these simulations, $\gamma_c = 0.01\gamma > \lambda, \kappa$, thus we are working in the weak coupling regime, yet we may still accomplish high-fidelity quantum interface operations.

In the above simulations we have assumed exact knowledge of the parameters $r(t)$, λ , κ , and γ . But in fact, there may be various errors in those parameters because of all kind of imperfections. Thus we need to evalu-

ate the influence of these errors on the fidelity of quantum interface operations. Table I shows the effects of the unknown errors in the various parameters on the fidelity of generating a single-photon wavepacket $\tilde{\alpha}(t)$, absorbing wavepacket $\tilde{\alpha}(t)$, and establishing entanglement $|\psi\rangle = \frac{1}{\sqrt{2}}(|d\rangle|vac\rangle + |g\rangle|\tilde{\alpha}(t)\rangle)$.

To examine the experimental feasibility of this proposal, considering the cantilever with the dimensions ($l = 100, w = 0.02, t = 0.01$) μm used in the literature [25] we adopt a silicon cantilever with a less demanding dimensions ($l = 50, w = 0.02, t = 0.01$) μm , which has a fundamental frequency $\omega_m \sim 3.516 \times (t/l^2) \sqrt{E/12\rho} \sim 2\pi \times 4.83$ kHz and $a_0 = \sqrt{\hbar/2M\omega_m} \sim 1.73 \times 10^{-11}\text{m}$, with the mass density $\rho \sim 2.33 \times 10^3 \text{kg/m}^3$, Young's modulus $E \sim 1.3 \times 10^{11}$ Pa, and the effective mass $M \sim \rho l w t / 4$ [22, 25]. A magnetic gradient of $G_m \approx 1.4 \times 10^6$ T/m generated by a magnetic tip with size of ~ 100 nm and homogenous magnetization $M_m \approx 2.3 \times 10^6$ T/ μ_0 at the distance $d_m \approx 25$ nm away from the tip was reported in [39]. Then we have a coupling strength $\lambda_0/2\pi = g_s \mu_B G_m a_0 / 2\pi \approx 0.68$ MHz. We set $\theta \approx 0.22\pi$ at the ‘‘sweet spot’’ and obtain $\lambda/2\pi \approx -0.43$ MHz [26, 40]. Note that in the numerical simulations we assume $\lambda/2\pi = 0.05$ MHz in Fig. 2, 3 and $\lambda/2\pi = 0.02$ MHz in Fig. 4. Here this minus ‘‘-’’ is not important, we can apply a unitary transformation $U = \exp(i\pi|d\rangle\langle d|)$ on the Hamiltonian (Eq. 18) to absorb it into $\hat{\sigma}_+$.

For an environmental temperature 10 mK and a quality factor $Q \sim 10^6$ the effective mechanical dissipation rate $\frac{k_B T}{\hbar Q} \approx 2\pi \times 0.21$ KHz. For the NV spin qubit we assume $\omega_q/2\pi = 0.7$ GHz, $\Delta/2\pi = -0.11$ GHz, and $\Omega/2\pi = 0.41$ GHz to meet the ‘‘sweet spot’’ condition $\theta \approx 0.22\pi$ where the quadratic corrections to the transition frequency ω_q vanish and results in a spin decoherence rate $\gamma_q/2\pi \approx 0.6 \times \delta_n^4 / (2\pi\omega_q^3) < 1$ Hz with $\delta_n \simeq 1$ MHz [26]. The drive amplitude can reach $-\Omega_p/2\pi \approx 8000$ GHz with the parameters $V_0 = 10\text{V}$, $V_p = 2\text{V}$, $A = 5\mu\text{m} \times 0.02\mu\text{m}$, and $d_e = 0.01\mu\text{m}$; while the maximum drive amplitude occurred in the simulation $-\Omega_p/2\pi \approx 7709$ GHz for the maximum squeezing parameter $r = 5$ (Fig. 4) and $\omega_q/2\pi = 0.7$ GHz. Concerning the optical parameters $\gamma_c/2\pi = 0.01\gamma$ and $\gamma/2\pi = 10$ MHz correspond to optical quality factor $Q_c \equiv \pi c / (\gamma \lambda_p) = 1.76 \times 10^7$ with $\lambda_p = 852$ nm [16, 31, 41]. Compared with $Q_c \geq 2 \times 10^9$ adopted in the seminal literature [16] to obtain state transfer fidelities $F \approx 0.85$, this scheme significantly relaxes the requirement on the cavity quality. As for the optomechanical coupling rate $\kappa/2\pi = 1.8$ MHz has been reported in the literature [28].

Now we discuss the RWA conditions. For the parameters $\dot{r}/2\pi \sim 5$ MHz (Fig. 2, 3, 4), $\kappa_{\text{ef}}/2\pi = 13.4$ MHz, $\lambda_{\text{ef}}/2\pi = 2.97$ MHz for $r = 5$, and $\omega_q/2\pi = \Delta_c/2\pi = 0.7$ GHz, the RWA conditions $\lambda_{\text{ef}}, \kappa_{\text{ef}}, \dot{r}/2 \ll \omega_q + \Delta_c$ are satisfied very well.

TABLE I. Effect of errors in parameters on the fidelities of generating a single-photon wavepacket $\tilde{\alpha}(t)$, absorbing such a wavepacket, and establishing entanglement $|\psi\rangle$. The evaluations are carried out by adding $\pm 10\%$ to the squeezing parameter $r(t)$, λ , κ , or γ respectively in the numerical simulations with other parameters remained the same as in figures 2, 3, 4.

	no error	10% $r(t)$ error	10% λ error	10% κ error	10% γ error
Generate	0.9862	0.8424	0.9801	0.9812	0.9873
Absorb	0.9869	0.8280	0.8975	0.9062	0.9446
Entangle	0.9841	0.9431	0.9515	0.9549	0.9788

V. CONCLUSIONS

We have described an experimentally feasible scheme to exponentially enhance the SM and OM coupling rates simultaneously through modifying a cantilever's

spring constant with a driving voltage. We have introduced an electrically-driven photon-spin quantum interface for quantum networks. Even in certain weak-coupling regime we can still design driving voltages to accomplish quantum state transfer and quantum entanglement distribution between two remote quantum nodes with high fidelity. Other than on NV spins the qubits may also be encoded on charge degrees of freedom [42]. The method may also find various applications in such as single-photon transistors [43], on-demand single-photon sources [44], and precise measurement of optically non-active quantum systems [45, 46].

ACKNOWLEDGMENTS

This work was supported by the National Natural Science Foundation of China (Grant No. 11872335) and by Zhejiang Provincial Natural Science Foundation of China (Grant No. Y6110314).

-
- [1] R.Hanson, F.M.Mendoza, R.J.Epstein, and D.D.Awschalom, *Phys.Rev.Lett.* **97**, 087601(2006); L.Childress *et al.*, *Science* **314**,281 (2006); T.Gaebel *et al.*, *Nat.Phys.***2**,408 (2006).
- [2] G. Balasubramanian *et al.*, *Nature Mater.* **8**, 383 (2009).
- [3] G.D. Fuchs *et al.*, *Science* **326**, 1520 (2009).
- [4] N.B. Manson, J.P. Harrison, and M.j. Sellars, *Phys. Rev. B* **74**, 104303 (2006).
- [5] C.H. Bennett and G.Brassard, in *Proceedings of the International Conference on Computers, Systems & Signal Processing* (Steering Committee, Bangalore, 1984),p. 175.
- [6] A. Broadbent, . Fittzsimons, and E. Kashefi, in *2009 50th Annual IEEE Symposium on Foundations of Computer Science* (IEEE, Atlanta, GA, USA, 2009),p.517 .
- [7] M. Caleffi *et al.*, Distributed quantum computing: A survey, **arXiv**, 2212.10609.
- [8] S. Simmons, *PRX QUANTUM* **5**, 010102 (2024).
- [9] P. Kómár *et al.*, *Nat.Phys.* **10**, 582 (2014).
- [10] Z. Zhang and Q. Zhuang, *Quantum Sci. Technol.* **6**, 043001 (2021).
- [11] J.I. Cirac *et al.*, *Phys. Rev. Lett.* **78**, 3221 (1997).
- [12] L.-M. Duan *et al.*, *Phys. Rev. A* **67**, 032305 (2003).
- [13] W. Yao *et al.*, *Phys. Rev. Lett.* **95**, 030504 (2005).
- [14] H. J. Kimble, *Nature (London)* **453**, 1023 (2008).
- [15] H. P. Specht, *Nature (London)* **473**, 190 (2011).
- [16] K. Stannigel *et al.*, *Phys. Rev. Lett.* **105**, 220501 (2010).
- [17] P.K. Shandilya *et al.*, *Nature Phys.* **17**, 1420 (2021).
- [18] K.C. Nowack *et al.*, *Science* **318**, 1430 (2007).
- [19] S. Asaad *et al.*, *Nature (London)* **579**, 205 (2020).
- [20] A. André *et al.*, *Nature Phys.* **2**, 636 (2006).
- [21] F. M. Hrubesch *et al.*, *Phys. Rev. Lett.* **118**, 037601 (2017).
- [22] P.-B. Li *et al.*, *Phys. Rev. Lett.* **125**, 153602 (2020).
- [23] X.-F. Pan *et al.*, *Phys. Rev. A* **107**, 023722 (2023).
- [24] X.-L. Hei *et al.*, *Phys. Rev. Lett.* **130**, 073602 (2023).
- [25] See the Supplemental Material at [http:// link.aps.org /supplemental /10.1103/PhysRevLett.130.073602](http://link.aps.org/supplemental/10.1103/PhysRevLett.130.073602) for more details.
- [26] P. Rabl,*et al.*, *Phys. Rev. B* **79**, 041302 (R) (2009).
- [27] G. Anetsberger *et al.*, *Nature Phys.* **5**, 909 (2009).
- [28] E. Verhagen *et al.*, *Nature (London)* **482**, 63 (2012).
- [29] K. Stannigel, P. Rabl, A. S. Sørensen, M. D. Lukin, and P. Zoller, *Phys. Rev. A* **84**, 042341 (2011).
- [30] M. L. Gorodetsky, A. D. Pryamikov, and V. S. Ilchenko, *J. Opt. Soc. Am. B* **17**, 1051 (2000).
- [31] S. M. Spillane, T. J. Kippenberg, O. J. Painter, and K. J. Vahala, *Phys. Rev. Lett.* **91**, 043902 (2003).
- [32] S. Mancini, D. Vitali, and P. Tombesi, *Phys. Rev. Lett.* **80**, 688 (1998).
- [33] T. A. Palomaki *et al.*, *Nature (London)* **495**, 210 (2013).
- [34] M. O. Scully and M.S. Zubairy, *Quantum Optics* (Cambridge University Press, 1997).
- [35] J.-M. Pirkkalainen *et al.*, *Phys. Rev. Lett.* **115**, 243601 (2015).
- [36] E.E. Wollman *et al.*, *Science* **349**, 952 (2015).
- [37] M.-A. Lemonde *et al.*, *Nat.Comm.* **7**, 11338 (2016).
- [38] See the Supplemental Material at [http:// link.aps.org /supplemental /10.1103/PhysRevLett.125.153602](http://link.aps.org/supplemental/10.1103/PhysRevLett.125.153602) for more details.
- [39] H. J. Mamin *et al.*, *Nature Nanotech.* **2**, 301 (2007).
- [40] F. Fung *et al.*, *Phys. Rev. Lett.* **132**, 263602 (2024).
- [41] S. M. Spillane, T. J. Kippenberg, K. J. Vahala, K. W. Goh, E. Wilcut, and H. J. Kimble, *Phys. Rev. A* **71**, 013817 (2005).
- [42] M. D. LaHaye *et al.*, *Nature (London)* **459**, 960 (2009).
- [43] D.E. Chang *et al.*, *Nature Phys.* **3**, 807 (2007).
- [44] B. Lounis *et al.*, *Rep. Prog. Phys.* **68**, 1129 (2005).
- [45] D. Rugar *et al.*, *Nature (London)* **430**, 329 (2004).
- [46] K. Jensen *et al.*, *Nature Nanotech.* **3**, 533 (2008).